A quasiclassical trajectory study of the time-delayed forward scattering in the hydrogen exchange reaction

Stuart J. Greaves,[a] Daniel Murdock,[b] and Eckart Wrede[c]
Department of Chemistry, University of Durham, South Road, Durham DHl 3LE, United Kingdom

(Received 10 May 2007; accepted 5 March 2008; published online 23 April 2008)

The time-delayed forward scattering mechanism recently identified by Althorpe *et al.* [Nature (London) **416**, 67 (2002)] for the $H+D_2(v=0,j=0)\rightarrow HD(v'=3,j'=0)+D$ reaction was analyzed by using quasiclassical trajectory (QCT) methodology. The QCT results were found to match the quantum wavepacket snapshots of Althorpe *et al.*, albeit without the quantum scattering effects. Trajectories were analyzed on the fly to investigate the dynamics of the atoms during the reaction. The dominant reaction mechanism progresses from hard collinear impacts, leading to direct recoil, toward glancing impacts. The increased time required for forward scattered trajectories is due to the rotation of the transient HDD complex. Forward scattered trajectories display symmetric stretch vibrations of the transient HDD complex, a signature of the presence of a resonance, or a quantum bottleneck state. © *2008 American Institute of Physics*. [DOI: 10.1063/1.2902973]

I. INTRODUCTION

The prototype hydrogen exchange reaction has been extensively studied, both theoretically and experimentally, creating a wealth of available literature (see, for instance, the recent review[1]). Recent experiments have been able to investigate the hydrogen exchange reaction in unprecedented detail, e.g., see Refs. 2–4, and along with quantum mechanical (QM) calculations, e.g., Refs. 5–7, the solution to this 80 year old problem may be in sight. There are still some topical aspects of the reaction that are currently discussed in the literature, not least the controversial topics of resonances[8] and quantum bottleneck states (QBSs).[9,10]

The accepted view is that the hydrogen exchange reaction is dominated by the direct recoil reaction mechanism, which involves a head-on collision with a linear transition state (TS); the bonds break and form concertedly and, due to the recoil from the collision, the products predominantly scatter in the backward direction. A recent experiment on the $H+D_2(v=0,j=0)\rightarrow HD(v'=3,j'=0)+D$ reaction observed a broad forward scattering peak. Corresponding time-dependent plane wavepacket calculations have identified a second distinct time-delayed reaction mechanism (delayed by 25 fs), which is the origin of this broad forward scattering peak.[11] The temporal and spatial separation of the mechanisms was demonstrated by using the snapshots from Althorpe's quantum wavepacket simulation of the reaction.[5,12] These simulations were able to reproduce time-of-flight data from the experiments of Ayers *et al.*[3] with good agreement; thus, it was concluded that the time delay in the calculations is real.[11]

Much of the controversy is focused on the mechanism(s) required for this time-delayed forward scattering. Some believe that it is due to Feshbach resonances, in which the H_3 collision complex is trapped in a well of an effective potential,[8,13] while others believe that QBSs, a series of effective reaction barriers at the TS, are responsible.[4,9,10] Note that the latter does not require a well in the effective potential and that, as in the classical analog, the time delay is caused by the slowing down of the atoms at the top of the effective barrier.[6]

Quasiclassical trajectory (QCT) calculations have long been used to understand the dynamics of chemical reactions. The classical picture for a direct reaction leading to forward scattering is the stripping mechanism. The incoming atom approaches the reactant molecule at large impact parameters and strips off an atom as it flies by and continues toward the forward region. Indeed, various quantum results show that forward scattering is exclusively due to partial waves with high total angular momentum J, which corresponds to high impact parameters.[4,9,11] Although the classical dynamics is unable to reproduce quantum effects such as interferences and tunneling and, thus, cannot reproduce certain experimental results accurately, QCT results are nonetheless in surprisingly good agreement with experimental and QM cross sections for this reaction,[2,8,14] which shows that the nuclear dynamics is predominately classical. In particular, we have recently demonstrated that the QCT method can give valuable insight into the motions of the nuclei during a reactive encounter and, thus, elucidate reaction mechanisms.[15,16] In this work, we will employ our recently developed tools to analyze trajectories and to discern the detail of the reaction mechanisms leading to forward scattering.

In Sec. II, we will briefly review our QCT methodology introduced in Ref. 16. The results of the QCT calculations and their comparison with QM snapshots will be discussed in

[a]Present address: School of Chemistry, University of Bristol, Bristol, BS8 1TS, UK.
[b]Present address: Department of Chemistry, Yale University, P.O. Box 208107, New Haven, CT 06520-8107.
[c]Author to whom correspondence should be addressed. Electronic mail: eckart.wrede@durham.ac.uk.

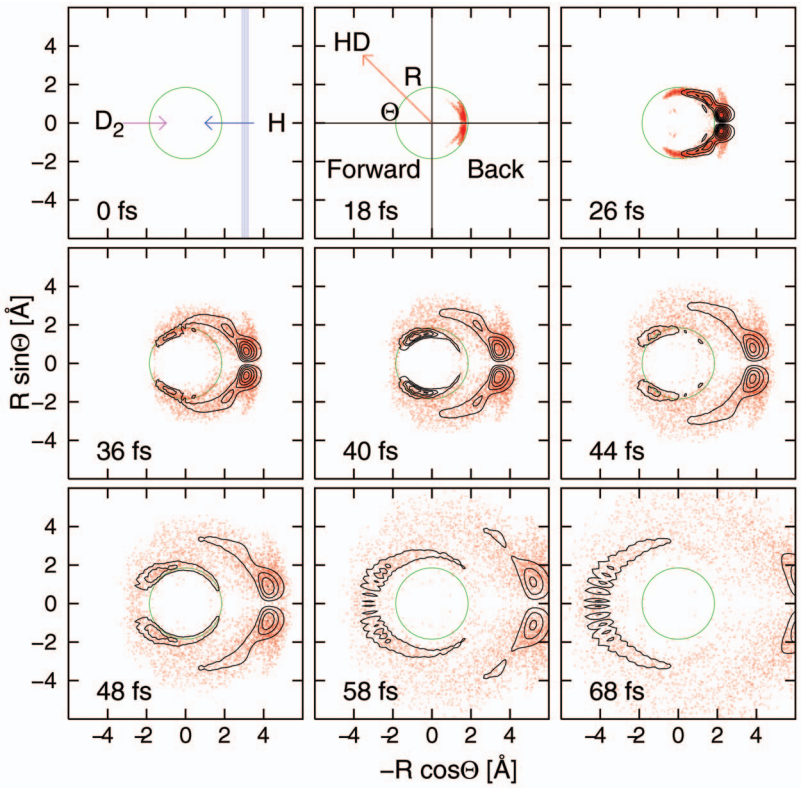

FIG. 1. (Color) Snapshots of the QCT $H+D_2(v'=0,j'=0)\rightarrow HD(v'=3,j'=0-1)+D$calculation over the energy range of 1.4–2.1 eV overlaid with contours from Althorpe's quantum wavepacket simulation of the $H+D_2(v=0,j=0)\rightarrow HD(v'=3,j'=0)+D$ reaction (Ref. 11). The contours are obtained from the complete wavefunction of the reaction and show the time evolution of the HD($v'=3$, $j'=0$) product as a function of the center-of-mass deflection angle Θ. The dashed circles are of radius $R=1.85$ Å and give a rough indication of the extent of the TS region. Two reaction mechanisms are visible in the contours separated by a time delay of about 25 fs. The height of the contours and the density of the dots indicate the quantity of HD($v'=3$, $j'=0-1$) molecules in that region.

Sec. III. Section IV describes our investigation into both backward and forward scattering mechanisms. Conclusions are given in Sec. V.

II. METHODOLOGY

The QCT methodology was adapted from Refs. 17 and 18 and is described in detail in Ref. 16. All the trajectories presented herein were propagated on the BKMP2 potential energy surface (PES)[19] by using the fixed stepsize Hamming predictor-corrector method[20] to integrate the equations of motion. The fixed integration stepsize was 3.5×10^{-17} s to ensure the conservation of the total energy and angular momentum to be better than 5 parts in 10^6 and 1 part in 10^7, respectively. The initial and final atom-diatom distance was 6 Å and the maximum impact parameter was 1.35 Å. The D_2 molecule was prepared in a discrete internal energy state corresponding to the initial quantum state of the molecule ($v=0$, $j=0$). The (v',j') quantum numbers of the outgoing molecule were assigned for a given rotational angular momentum by equating the internal energy to the full Dunham expansion of the rovibrational energies of the HD molecule.[21]

An advantage of the QCT method is the ability to differentiate between near-side (the positive y-hemisphere, i.e., the same side as the impact parameter, see Fig. 2 of the adjacent paper[16]) and far-side (the negative y-hemisphere) scattered products. Thus, we define the deflection angle Θ as the positive scattering angle, $\Theta=+\theta_{\text{scatt}}$, for near-side scattering and the negative scattering angle, $\Theta=-\theta_{\text{scatt}}$, for far-side scattering.

III. RESULTS

A. Reproducing quantum snapshots

Outcomes of QCT calculations were compared to snapshots of the QM wavepackets derived from calculations of Althorpe. The QM snapshots were produced by projecting the total wavefunction onto a HD(v',j') product wavefunction to obtain a function that describes when and where the HD(v',j') product is formed and how it scatters.[12]

A trajectory was deemed to have progressed to a state where the product molecule is formed after the first minimum in the H–D internuclear distance (inner turning point of HD product vibration). The position of the HD center of mass is calculated as a function of the D–HD distance R and deflection angle Θ relative to the initial direction of the H atom (plots will be shown in planar polar coordinates $R\sin\Theta$ versus $R\cos\Theta$), at the closest integration step to the specific times used in Ref. 11. These data are shown in a density plot, in direct comparison to Althorpe's quantum wavepacket contours in Fig. 1, where the HD product densities are represented by the height of the contours and the density of the dots. Due to the ability of QCT calculations to distinguish between near- and far-side scattering, the QCT snapshots are mirrored in $R\sin\Theta=0$ for ease of comparison with the QM snapshots.

The QM snapshots used an energy range of 1.3–2.1 eV with a flat distribution damped to zero at the edges.[11] QCT snapshots for HD($v'=3$, $j'=0$) were produced by calculating a batch of trajectories using a randomly selected collision energy over the range $E_{\text{col}}=0.9-2.1$ eV. The QCT trajectories that were in the energy range of 1.4–2.1 eV were used to compare with the quantum picture, as the threshold for the $v'=3$ state is 1.4 eV. 8 750 000 trajectories were run of

which only 793 resulted in the HD($v'=3$, $j'=0$) quasiquantum state. To enlarge the statistical sample for comparison, the 3066 trajectories in the HD($v'=3$, $j'=0-1$) quasiquantum states were used, as the extra rotation had very little effect upon the distribution of the products in the snapshots.

B. QM comparison

Figure 1 shows that the QCT calculations match the general temporal and spatial trend in the contours. Backward scattered products are formed first and have the greatest density. The gap at $\Theta=180°$ reflects the fact that central collinear collisions are least likely. The "arms" leading from backward to sideways scattering are also seen in both cases. In both methodologies, the forward scattered products were formed last and move further around the TS region toward each other. In the QM snapshots, this causes a quantum interference pattern, which is an example of the glory effect,[22–24] that is not seen in the forward scattered QCT products.

While the general trends of the QCT calculations are the same, the complete separation of the time-delayed forward and fast backward mechanisms, as apparent in the QM snapshots (40 fs frame of Fig. 1), is not seen in the QCT calculations. The QCT result shows none of the enhanced intensity in the TS region (shown as the central circle in each frame) in the 40 fs frame. This may be due to the QM methodology in which the snapshots are produced by projecting the total wavefunction onto a HD(v',j') product wavefunction;[12] thus, recrossing trajectories may also be included in the product density. Only trajectories that scatter to the HD($v'=3$, $j'=0-1$) product state have been used to reproduce the QM snapshots, so densities in the TS region may not be comparable.

While the bulk of the QCT picture matches the QM, the QCT picture lacks definition. Better resolution was required to discern the classical reaction mechanisms that govern the scattering into the HD($v'=3$, $j'=0-1$) product states.

C. Refining the QCT picture

Our recent work examining the HD($v'=0$, $j'=0$) products of this reaction[16] greatly benefited from the use of a single collision energy and restricted product quasivibrational state to give the reaction products the same recoil speed. The following restrictions on initial and final conditions for the QCT calculations presented here were used to clarify the scattering dynamics of the HD($v'=3$, $j'=0-1$) products. Fixed collision energy: The use of a single collision energy gave the product molecules in any given quantum state the same relative product kinetic energy E_{col} and, therefore, speed. Thus, the time dependence of the trajectories is more clearly defined in the snapshots. Fixed collision energies of 1.49, 1.64, and 1.85 eV were selected to match experimental studies,[11] and $E_{col}=2.1$ eV was used to match the upper energy limit of the QM snapshots. Calculations were carried out at these collision energies by using the same QCT parameters. Restricted product quantum state: The QCT method generates continuous product state quantum numbers, which are usually rounded to the nearest integer (histogram binning method), e.g., $v'_{QCT}=3.5-4.5$ is assigned to $v'=3$. Consequently, each quasiclassically assigned quantum state has a range of internal energies and, therefore, a corresponding spread of product velocities. To clarify the time dependent evolution of trajectories and the following identification of novel reaction mechanisms, only trajectories with a vibrational quasiclassical quantum number in the range $v'_{QCT}=3.9-4.1$ were analyzed.

TABLE I. QCT calculation results for a range of collision energies, showing the total number of trajectories calculated, the number that are reactive, and the number that result in the HD($v'=3$, $j'=0-1$) quasiquantum states.

E_{col} (eV)	Dimensionality	Total	Reactive	$v'=3$, $j'=0-1$
2.10	2D	1 000 000	288 003	1785
1.85	2D	1 000 000	298 819	2300
1.85	3D	5 000 000	1 082 947	3346
1.64	2D	1 000 000	300 125	2266
1.64	3D	1 000 000	210 992	511
1.49	3D	1 000 000	203 834	279

D. Results

The results of the QCT calculations are summarized in Table I. Figure 2 shows snapshots created by using a single collision energy (1.85 eV), restricted final quantum state, and trajectories initiated in the yz-plane [i.e., all three atoms are restricted to the same plane as the impact parameter, see panel (a) of Fig. 3]. The use of this two dimensional restriction improves the clarity of the snapshot and, thus, the underlying dynamics. Analysis of the three dimensional (3D)

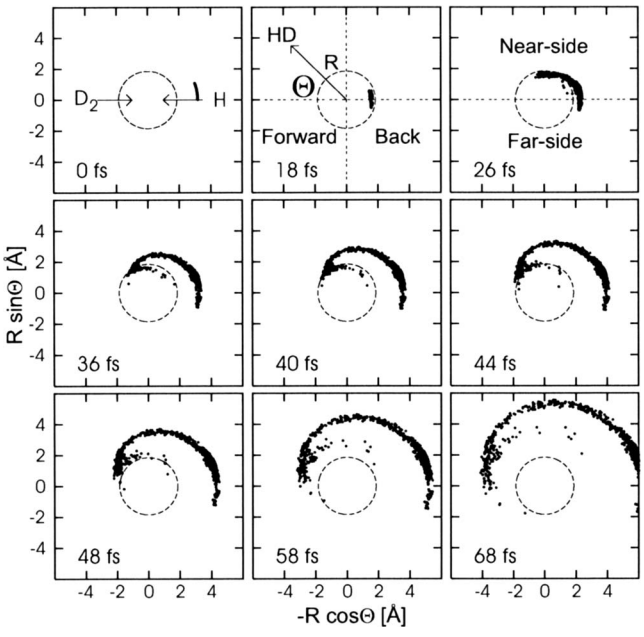

FIG. 2. Snapshots of the HD product densities for $H+D_2(v'=0,j'=0) \rightarrow HD(v'=3,j'=0-1)+Dat$ $E_{col}=1.85$ eV restricted to the yz-plane. Each point represents the position of a HD product for a single trajectory. The central circle gives an indication of the size of the interaction region, and the arrow in panel 18 fs is pointing in the forward scattered direction. The trajectories have not been symmetrized, as in Fig. 1, and the near- and far-side scattering regions are delineated in panel 26 fs. The spiral shows the continuation from backward to forward scattering.

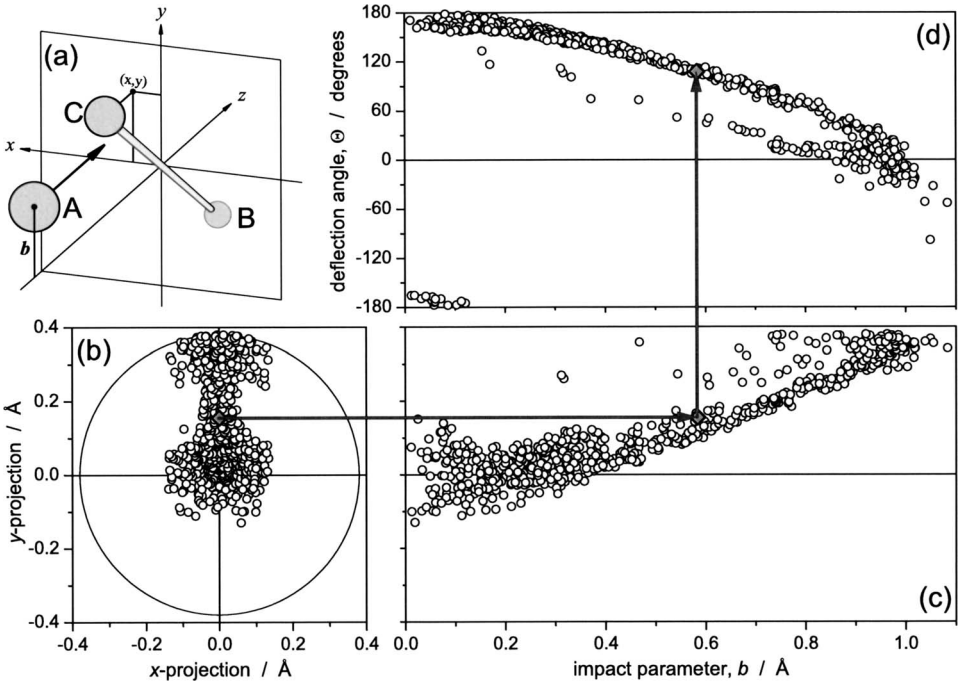

FIG. 3. Plots showing the correlation between impact parameter b, D_2 axis orientation, and deflection angle Θ, and correlation for the HD($v'=3$, $j'=0-1$) products at $E_{col}=1.85$ eV. (a) Initial conditions for a trajectory: Impact parameter b and location of the leading D atom projected onto the xy-plane shown in panel (b), see text for details. (c) Correlation between the impact parameter and the initial y-coordinate of the leading D atom. (d) Correlation between the impact parameter and deflection angle. The forward scattering region, $\Theta<30°$, can only be accessed with the highest impact parameters. A collinear trajectory would be represented by a point at (0,0) in panel (b) with zero impact parameter in panel (c) and a deflection angle of 180° in panel (d). A forward scattering trajectory would be represented by a point at $x=0$ and on the top of the circle in (b) with an impact parameter of 0.9 Å and a deflection angle of 0°.

trajectories found that for deflection angles between 0° and 150°, the system is very planar, making this restriction appropriate. The remainder of the analysis will only consider full 3D trajectories.

The trajectories in the snapshots have not been mirrored in $R \sin \Theta=0$; thus, trajectories that scatter into the far-side region can be discerned (as labeled in the bottom half of the 26 fs frame in Fig. 2). Figure 2 shows a much "sharper" picture when compared to Fig. 1; the main scattering feature is shown to have a spiral form leading from backward to forward scattering with a smaller inner branch, which can be seen inside the central circle in the 40 fs frame. The main spiral feature was also observed for each of the other energies studied.

IV. ANALYSIS AND DISCUSSIONS

A. Investigations into mechanisms

The accepted view is that backward scattered products form via a direct recoil mechanism, which is collinear at attack. QCT calculations have previously shown that forward scattering requires a large impact parameter for a glancing attack.[25,26] It was shown that high J values in QM calculations, the equivalent of large impact parameters in QCT, also give rise to forward scattering.[9,11] Both the direct recoil and glancing attack mechanisms can only originate from highly correlated initial conditions, e.g., all the atoms have to be aligned for direct recoil.

In the following sections, the correlations of initial conditions will be investigated along with an analysis of how the hydrogen atom "impacts" on the steep repulsive potential around the D_2. The impact and recoil mechanisms can be confirmed by the analysis of the configuration of the atoms at the point of impact, and the angle of the impact from the path of the incoming H atom, which heavily relies on the initial orientation of the system.

To investigate the forward scattering mechanism, the motion of the system in the TS region was examined and a measurement of the time delay was implemented. The analysis of the TS region informed much of the other areas of analysis, and as such the following sections cannot be seen as independent but should be viewed as a whole.

B. Impacts

To test the supposition that glancing impacts give rise to sideways and forward scattering, the configurations of the atoms at the point of first impact were examined. An impact can be defined as a maximum in the potential energy and, thus, a minimum in the kinetic energy, of the HD_2 system. An adjusted potential was devised to remove the current (as defined by the smallest internuclear distance at that time step) molecular vibration from the total potential.[16] The relative positions of the three atoms were recorded at the first impact point, defined as the first maximum in the adjusted potential. This allowed the creation of an "impact diagram"; the overlay of the paths of the atoms onto a Cartesian contour plot of the PES at the point of impact.

The direct recoil mechanism proceeds via a single hard impact on the outside of the D_2 with a collinear arrangement at impact. Direct recoil, which leads to "backward scattering" of the HD products, is thought to make up the bulk of all reactive trajectories. This mechanism clearly explains the trajectories that scatter backward; we will now show how a trajectory scatters sideways.

The correlations between the initial geometry defined by the orientation of the D_2 axis and the impact parameter b and the HD product's deflection angle are shown for trajectories that lead to HD($v'=3$, $j'=0-1$) in Fig. 3. The orientation of the D_2 molecular axis is plotted as the projection of the leading D atom onto the xy-plane, as depicted in panel (a) of Fig. 3. To eliminate the effect of the vibrational motion, we plot this projection for the fixed D_2 equilibrium bond length. Ini-

tial D_2 orientations perpendicular to the direction of the incoming H atom would lie on the circle in panel (b) and orientations along the z-axis at the origin. Panel (c) shows the correlation between the y-coordinate of the projection and the impact parameter. A collinear trajectory would be represented by a point at the origin in panel (b) and a point at zero impact parameter in panel (c). Finally, the correlation between the impact parameter and the deflection angle is shown in panel (d). The two arrows in Fig. 3 highlight a single trajectory (gray diamond) that scatters sideways ($\Theta = 107°$) due to its impact parameter (0.58 Å) and the y-projection (0.154 Å) of its leading D atom.

The correlations between initial conditions and deflection angle for trajectories that lead to HD($v'=3$, $j'=0-1$) shown in Fig. 3 demonstrate that a single continuous mechanism is responsible for the scattering into the main spiral from backward to forward directions. This is caused by the impact parameter b concertedly increasing with the D_2 axis orientation. The trajectories are shown to be near planar in nature; the yz-plane has an x-coordinate of zero in panel (b). The forward scattering region, $\Theta < 30°$, can only be accessed with the highest impact parameters and a perpendicular D_2 axis.

The implications of the correlation highlighted by Fig. 3 for the impact mechanism of backward scattering can be seen for a range of deflection angles in the impact diagrams in Fig. 4. The "RR plots" on the right hand side of Fig. 4 show the trajectories in the product (horizontal) and reactant (vertical) channels of the PES (shown at the bending angle on impact); the barrier is the diagonal dashed line. Motion of the hydrogen atom along or parallel to this line indicates a symmetrical stretching of the atoms. The dashed line box in the lower left hand corner of the RR plots is the interaction or the TS region. The trajectory is said to be in the TS region if both the (smallest) H–D and D–D distances are below the symmetric stretch threshold, defined as the maximum symmetric stretch separation possible at the given total energy, i.e., the largest possible values of R_{H-D} and R_{D-D} while in a linear symmetric ($R_{H-D}=R_{D-D}$) stretch. It has the advantage of scaling with collision energy so trajectories with different collision energies can be compared.

The impact diagrams on the left hand side of Fig. 4 also contain information about the rotation of the HD_2 complex; the motion of the D atoms (dotted lines) show sharp bends between the D_2 vibrational axis and the direction of separation of HD and D products. These bends indicate the magnitude of the rotation of the complex. The trajectories shown in Fig. 4 are typical of the scattering regions indicated.[27]

The following is a description of selected trajectories shown in Fig. 4. Backward ($\Theta=180°$): A low impact parameter and collinear attack result in direct recoil with no rotation of the complex. The RR plot shows that the trajectory quickly passes through the interaction region with no complex excitation. Sideways ($\Theta=90°$): In this glancing impact trajectory, the H atom approaches with a larger impact parameter and the D_2 axis is angled for an end-on impact, causing some rotation of the complex. The RR plot shows that this trajectory is slightly delayed in the interaction region, with the first maximum of the product vibration lying within the interaction region. Forward ($\Theta=0°$): For this glancing impact trajectory, the H atom approaches at a very large impact parameter with the D_2 axis nearly perpendicular causing a glancing deflection of the H atom off the repulsive potential close to the D_2 and a large rotation of the complex. The RR plot shows that longer delay in the interaction region involves a prominent symmetric stretch motion (R_{AB} and R_{BC} concertedly expand and contract) compared to backward and sideways scattering.

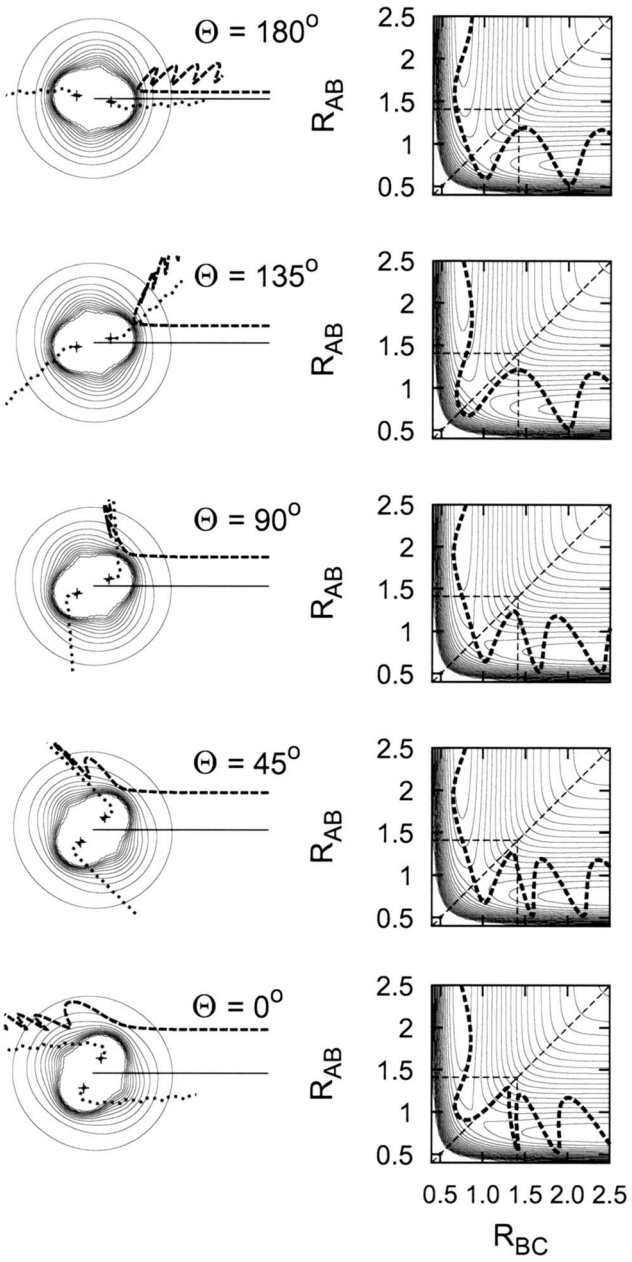

FIG. 4. Direct visualization of the geometry at impact. Impact diagrams (left): Using the space-fixed frame, we show the position of the atoms and the PES in Cartesian coordinates at the point of impact. The dotted lines represent the motion of the D atoms; H atoms (dashed line) approach from the right. RR plots (right) show the trajectories in the product and reactant channels of the PES, and the barrier is the diagonal dashed line. Motion of the hydrogen atom along or parallel to this line indicates a symmetrical stretching of the atoms. The coordinates are reactant (R_{BC}) and product (R_{AB}) bond lengths; trajectories start from the top left hand side of the plot (R_{BC} small) and the interaction region is represented by the dashed line box in the lower left hand corner (see text for details of individual trajectories).

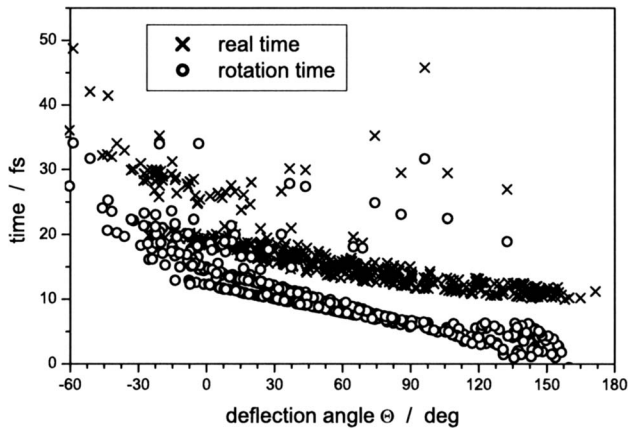

FIG. 5. Correlation between time and deflection angle. Real time spent in the interaction region (×) compared to the minimum time required for complex rotation t_{rot} (○) as a function of deflection angle Θ.

C. Complex rotation

The magnitude of rotation displayed in impact diagrams in Fig. 4 is correlated with the deflection angle Θ. The correlation between rotation time (t_{rot}) and deflection angle is shown along with the time spent in the interaction region (defined by the symmetric stretch threshold) in Fig. 5. The rotation time is defined as the minimum time required for the complex to rotate between its initial and final angles. These initial and final angles are given by the hydrogen's initial approach vector and the products' scattering vector (which define the scattering plane), the angle between which is the deflection angle Θ. The angular velocity vector $\vec{\omega}$ was calculated by using the moment of inertia tensor $\mathbf{I}$ of the complex at the closest approach of the three atoms and the total angular momentum of the system, $\vec{L}$, (governed only by the impact parameter for that trajectory, as in this case $j=0$),

$$\vec{\omega} = \mathbf{I}^{-1}\vec{L}. \tag{1}$$

$\vec{\omega}$ is then projected onto the normal vector of the scattering plane (which defines the axis around which the complex has to rotate to get from the initial vector of approach to the final vector of product recoil) to calculate the required speed of rotation, ω. The rotation time t_{rot} is then given by

$$t_{rot} = \theta_{rot}/\omega, \tag{2}$$

where the rotation angle is given by $\theta_{rot}=180-\Theta$.

It can be seen in Fig. 5 that for trajectories in the main spiral scattering feature, the major contribution to the time spent in the interaction region is the time required for the rotation of the HD_2 complex. Similar time delays were seen in classical trajectory calculations that accompanied the QBS analysis reported by Harich *et al.*[9] A small part of the longer time taken by forward scattering trajectories can be attributed to the extra distance that has to be traveled and the extra time it takes to make the first impact.

The glancing impact mechanism, where the H atom glides off the end of the D_2, is a natural progression from backward recoil. With higher impact parameters and the correct initial orientations, it can lead to a continuous range of center-of-mass scattering angles from backward to forward. This continuous nature was also shown in the snapshots of Fig. 2 as an unbroken spiral. High impact parameters and glancing impact have been suspected of exclusively leading to forward scattering trajectories in a separate mechanism,[11] but here it is shown to be part of a continuous classical mechanism from backward to forward scattering. The time delay between backward and forward scattering is simply due to the time it takes the HDD complex to rotate.

The longer time delays seen in Fig. 5 (>21 fs) that make up the inner branch of the spiral (inside the circle in the 40 fs frame of Fig. 2) are not exclusively caused by rotation; a more complex mechanism is at work. It has been suggested that a glancing attack mechanism would have to convert energy initially concentrated in the HDD bend into energy along the HDD asymmetric stretch to allow the system to pass over the TS and react.[11] If the energy was initially converted into a symmetric stretch, then the HDD complex would be "trapped" in the TS for the period of that stretch. It has already been shown (Fig. 4) that the forward scattered products can undergo a symmetric stretch (R_{AB} and R_{BC} concertedly expand and contract) in the TS region. Analysis of the TS behavior of trajectories was thus conducted to ascertain the importance of these observations.

D. Transition state behavior

The behavior of trajectories at the TS is of great interest,[26,28] and can be used to explain time delays[11] found in calculations. Short-lived complexes at the TS are often attributed to resonances in reactive scattering.[26]

QCT calculations have been used to estimate the time the system spends in the TS region, the time delay of the trajectory. Long time delays have been attributed to trapping in a bending motion,[26] or trapping in a symmetric stretching motion.[28] The time delay of a trajectory is, in general, an ill defined concept, and previous attempts have used arbitrary measurements, some of which were affected by the different recoil speeds that are dependent on the product state.[26]

Our time delay is defined as the time between the (smallest) R_{H-D} coordinate going below the symmetric stretch threshold and the time the R_{DD} goes above this threshold for the last time. This provided an indication of the amount of time spent in the interaction region where trapping is possible.

1. Symmetry coordinates

To analyze the trajectories in the TS, the three internal coordinates of HDD (r_1 and r_2 are the distances from the center atom to each of the end atoms and θ_b is the angle between r_1 and r_2) were used to calculate the following symmetry coordinates:[29] Symmetric stretch s_1, bending s_2, and antisymmetric stretch s_3,

$$s_1 = \frac{\Delta r_1 + \Delta r_2}{\sqrt{2}}, \tag{3a}$$

$$s_2 = \sqrt{(r_1 r_2)}\Delta\theta_b, \tag{3b}$$

$$s_3 = \frac{\Delta r_1 - \Delta r_2}{\sqrt{2}}. \tag{3c}$$

In Eq. (3) $\Delta r_1 = r_1 - r_e$, $\Delta r_2 = r_2 - r_e$, and $\Delta\theta_b = \theta_b - \theta_e$, where $r_e = 0.929\,76$ Å and $\theta_e = 180°$ are the equilibrium values at the TS. Note that the antisymmetric stretch corresponds to motion along the minimum energy path over the reaction barrier. These coordinates were recorded over the course of the trajectory and used to determine if there was trapping in these motions at the TS.

Trapping was, for our purposes, defined as a time delay caused by a symmetric stretching motion. A symmetric stretch is defined as $R_{AB} \simeq R_{BC}$ concertedly expanding, reaching a maximum, and, at least in part, contracting together. A trajectory was said to undergo a symmetric stretch when at least two minima and one maximum in the symmetric coordinate were recorded under the stretching threshold. Multiple stretches were assigned if a greater number of minima and maxima were recorded. The sign of the antisymmetric stretch coordinate during a symmetric stretch was used to discern if trapping occurred in the reactant or product channel.

The bending coordinate was found to correlate to the other symmetry coordinates for certain trajectories, but its interaction with the other coordinates was complex and could not be easily quantified. As the stretching coordinates and rotation were adequate to describe the complex motion in the TS region, the bending coordinate is not considered in this analysis.

The degree of trapping a trajectory experiences was described by the following generalized criteria (used for all trajectories at all energies). Not trapped: A direct trajectory that moves quickly across the TS and, therefore, has a short time delay. Insertion mechanism leading to two TS paths: $A+BC \rightarrow A-BC \rightarrow B-A-C \rightarrow B+AC$; this mechanism, which accounts for 0.1% of reactive scattering, is not considered in this report, but it is important to exclude these trajectories so they do not confuse the analysis of other mechanisms. More detail about this mechanism can be found in Ref. 15. Trapped in the product channel: The symmetric coordinate shows a large stretch, while the antisymmetric coordinate is zero. Trapped in the reactant channel: During the symmetric stretching motion, the antisymmetric stretch coordinate becomes negative. This indicates that the trajectory has recrossed the reaction barrier back into the reactant channel. Trapped with multiple symmetric stretches: The symmetric stretch coordinate has a series of maxima and minima indicating the multiple stretching motions; they have been previously observed by Muga and Levine.[28] These are the longest lived trajectories, but with only a few trajectories per quantum state, the contribution to the final classical cross section is small. These trajectories make up the inner branch of the spiral and scatter to a wide range of angles and as shown on the interaction region circle in the 44 fs frame of Fig. 2.

For a direct trajectory, little time is spent in the interaction region, so its time delay is small (≈16 fs), but for a trajectory that goes through a single symmetric stretch motion the time delay is significantly larger (≈33 fs); for a multiple stretching trajectory, the time delay is 62 fs or more.

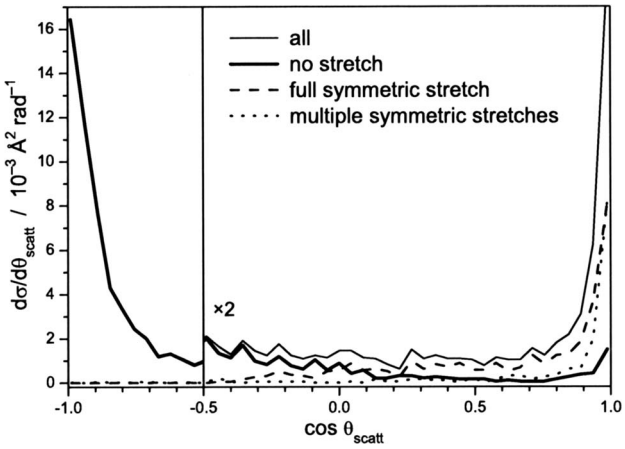

FIG. 6. Complex excitation as a function of scattering angle. Almost all the forward scattered trajectories, $\theta_{scatt} < 40°$, $\cos\theta_{scatt} > 0.75$, undergo at least one full symmetric stretch, whereas all the backward trajectories display no stretch.

This study has shown that forward scattered trajectories display a significant amount of symmetric stretch vibration of the HDD complex.

2. The importance of trapping

For QCT, the reactive cross section for a batch of trajectories is given by[17]

$$\sigma = \pi b_{\max}^2 \frac{n}{N}, \tag{4}$$

where $b_{\max}$ is the maximum impact parameter sampled (1.35 Å), n is the number of trajectories with a given property [e.g., scattered into a given HD(v',j') quantum state or having a number of symmetric stretches], and N is the total number of trajectory run.

The differential cross section (DCS) in Fig. 6 demonstrates the contribution of symmetric stretching trajectories to the forward scattering region of the HD($v'=3$, $j'=0-1$) product states, using a histogram binned in the cosine of the scattering angle and Eq. (4). The results for 5×10^6 three dimensional trajectories (without quasi-v' restriction) carried out at $E_{col} = 1.85$ eV were used for the calculation of the DCS. Backward scattered trajectories, $\cos\theta_{scatt} < -0.5$, exhibit minimal contribution from symmetric stretches. As the scattering angle decreases, the number of trajectories undergoing symmetric stretch vibrations of the HDD complex increases. These "vibrations" could be caused by the motion of the H flying past the D_2 during the first glancing impact, as shown in Fig. 4 ($\Theta = 0°$).

V. CONCLUSIONS

Results from a QCT study into the hydrogen exchange reaction for the $H+D_2$ isotopic variant have been presented. The results were compared to recent QM calculations[11] and used to elucidate reaction mechanisms in the HD($v'=3$, $j'=0-1$) product state.

QCT calculations have been demonstrated to be a good match for the temporal and spatial trends in the contours of the QM snapshots (see Fig. 1), including the time delay be-

tween forward and backward scattered products. However, the temporal separation between forward and backward scattering or interferences from glory scattering cannot be observed in QCT. It is proposed that both of these quantum effects can be justified as interferences between two independent classical trajectories that lead to the same scattering angle.[30] The glory scattering derives from the time-delayed trajectories of the inner branch of the spiral moving around the interaction region from sideways to forward scattering angles and interfering in the forward region. These trajectories display a significant amount of symmetric stretch vibration of the HDD complex; indeed, the majority undergo multiple stretches and some even show longer term excitation, as previously observed by Muga and Levine.[28] The temporal separation between forward and backward scattering in the QM picture could be seen as an interference between the fast glancing trajectories that scatter sideways and the multiple stretching (trapped) trajectories that scatter into the same sideways region. QCT cannot detect resonances or QBSs, but the symmetric stretches and bends described here for the forward scattered trajectories are consistent with the complex motions predicted for both resonances[13] and QBS.[4,10]

The dominant classical mechanism, which controls scattering into the outer spiral of the QCT snapshots (Fig. 2), progresses from hard collinear impacts to glancing impacts. The increased time for the sideways and forward scattered trajectories is due to the rotation of the HDD complex and extra distance traveled by the H atom. This mechanism derives from the strong correlations between the initial orientation of the D_2 axis and impact parameter, which determines the deflection angle. The $v'=3$ product state is excited by hard impacts at the inner turning point of the $v'=3$ vibration. For the glancing impacts, the closest approach of the hydrogen does not allow this direct excitation, but the subsequent motion of the atoms, especially if in a symmetric stretch, provides excitation to the $v'=3$ state through the outer turning point of the $v'=3$ vibration.

The QCT method has been shown to give valuable insight into the simplest chemical reaction. By examining individual quantum states, finding correlations between initial conditions, and using simplified reaction systems, reaction mechanisms have been discerned. This method has the ability to graphically demonstrate the reaction mechanisms that can lead to interference phenomena in QM calculations.

ACKNOWLEDGMENTS

We thank S. C. Althorpe for the use of his quantum snapshots and for helpful discussions. S.J.G. acknowledges the funding of a studentship by EPSRC and the Department of Chemistry, University of Durham. We thank the EPSRC for financial support.

[1] F. J. Aoiz, L. Bañares, and V. J. Herrero, Int. Rev. Phys. Chem. **24**, 119 (2005).
[2] E. Wrede, L. Schnieder, K. H. Welge, F. J. Aoiz, L. Bañares, V. J. Herrero, and B. Martínez-Haya, J. Chem. Phys. **110**, 9971 (1999).
[3] J. D. Ayers, A. E. Pomerantz, F. Fernández-Alonso, F. Ausfelder, B. D. Bean, and R. N. Zare, J. Chem. Phys. **119**, 4662 (2003).
[4] D. X. Dai, C. C. Wang, S. A. Harich, X. Y. Wang, X. M. Yang, S. D. Chao, and R. T. Skodje, Science **300**, 1730 (2003).
[5] S. C. Althorpe, Int. Rev. Phys. Chem. **23**, 219 (2004).
[6] L. Bañares, F. J. Aoiz, and V. J. Herrero, Phys. Scr. **73**, C6 (2006).
[7] M. Hankel, S. C. Smith, R. J. Allan, S. K. Gray, and G. G. Balint-Kurti, J. Chem. Phys. **125**, 164303 (2006).
[8] F. Fernández-Alonso, B. D. Bean, J. D. Ayers, A. E. Pomerantz, R. N. Zare, L. Bañares, and F. J. Aoiz, Angew. Chem., Int. Ed. **39**, 2748 (2000).
[9] S. A. Harich, D. X. Dai, C. C. Wang, X. M. Yang, S. D. Chao, and R. D. Skodje, Nature (London) **419**, 281 (2002).
[10] R. T. Skodje and X. M. Yang, Int. Rev. Phys. Chem. **23**, 253 (2004).
[11] S. C. Althorpe, F. Fernández-Alonso, B. D. Bean, J. D. Ayers, A. E. Pomerantz, R. N. Zare, and E. Wrede, Nature (London) **416**, 67 (2002).
[12] S. C. Althorpe, J. Chem. Phys. **117**, 4623 (2002).
[13] T. C. Allison, R. S. Friedman, D. J. Kaufman, and D. G. Truhlar, Chem. Phys. Lett. **327**, 439 (2000).
[14] F. J. Aoiz, L. Bañares, M. J. D'Mello, V. J. Herrero, V. Sáez Rábanos, L. Schnieder, and R. E. Wyatt, J. Chem. Phys. **101**, 5781 (1994).
[15] J. C. Juanes-Marcos, S. C. Althorpe, and E. Wrede, J. Chem. Phys. **126**, 044317 (2007).
[16] S. J. Greaves, D. Murdock, E. Wrede, and S. C. Althorpe, J. Chem. Phys. **128**, 164306 (2008).
[17] D. G. Truhlar and J. T. Muckerman, in *Atom-Molecule Collision Therory: A Guide for the Experimentalists*, edited by R. B. Bernstein (Plenum, New York, 1979), pp. 505–566.
[18] F. J. Aoiz, V. J. Herrero, and V. S. Rábanos, J. Chem. Phys. **94**, 7991 (1991).
[19] A. I. Boothroyd, W. J. Keogh, P. G. Martin, and M. R. Peterson, J. Chem. Phys. **104**, 7139 (1996).
[20] A. Ralston and H. Wilf, *Mathematical Methods for Digital Computers* (Wiley, London, 1960).
[21] L. Bañares, F. J. Aoiz, P. Honvault, B. Bussery-Honvault, and J.-M. Launay, J. Chem. Phys. **118**, 565 (2003).
[22] D. Sokolovski, Chem. Phys. Lett. **370**, 805 (2003).
[23] J. N. L. Connor, Phys. Chem. Chem. Phys. **6**, 377 (2004).
[24] S. C. Althorpe, J. Chem. Phys. **121**, 1175 (2004).
[25] D. G. Truhlar and R. E. Wyatt, Annu. Rev. Phys. Chem. **27**, 1 (1976).
[26] F. J. Aoiz, V. J. Herrero, and V. S. Rábanos, J. Chem. Phys. **97**, 7423 (1992).
[27] Animations of trajectories of the mechanisms described in this paper can be accessed at http://www.durham.ac.uk/eckart.wrede/QCT/forward/.
[28] J. G. Muga and R. D. Levine, Chem. Phys. Lett. **162**, 7 (1989).
[29] P. F. Bernath, *Spectra of Atoms and Molecules* (Oxford University Press, Oxford, 1995).
[30] R. D. Levine and R. B. Bernstein, *Molecular Reaction Dynamics and Chemical Reactivity* (Oxford University, Oxford, 1987).